

## Estimation of Effective Surface Area: A Study on Dolomite Cement Dissolution in Sandstones

Jin Ma, Martin O. Saar, Xiang-Zhao Kong\*

Geothermal Energy and Geofluids Group, Department of Earth Sciences (D-ERDW), ETH-Zürich, CH-8092, Switzerland

\*xkong@ethz.ch

**Keywords:** Dissolution, Dolomite, Effective surface area

### ABSTRACT

Fluid-rock reaction plays a critical role in many natural and/or engineered hydrogeological processes. It is well-known that the reaction rate highly depends on the effective surface areas (ESA) of minerals that participate in the reactions. However, quantifying the ESA has been reported to be challenging. In this study, we analyzed the ESA of dolomite cement ( $\text{Ca}_{1.05}\text{Mg}_{0.75}\text{Fe}_{0.2}(\text{CO}_3)_2$ ) in a multi-mineral sandstone from a geothermal formation. We first combined BET gas absorption measurements with high resolution SEM-EDS ( $1.2\ \mu\text{m}$ ) image processing, to obtain the physically accessible surface area (ASA) of the dolomite cement, which was  $0.065\ \text{m}^2/\text{g}$ . Then, we delineated the ESA evolution during the dissolution of the dolomite cement, by performing a reactive flow-through transport experiment under reservoir conditions. We circulated  $\text{CO}_2$ -enriched brine through the specimen for 137 cycles ( $\sim 270$  hours) to examine the evolution of in-situ hydraulic properties and  $\text{CO}_2$ -based geochemical fluid-rock reactions, with the focus on the dissolution of dolomite cement. Water chemistry analyses on the effluent samples yielded a sample-averaged ESA of  $8.86 \times 10^{-4}\ \text{m}^2/\text{g}$  and an effective coefficient of the reactive surface area for dolomite of  $1.36 \times 10^{-2}$ , indicating a limited participation of the physical surface area. As the dissolution reaction progressed, the ESA was observed to first increase, then decrease. Our results provide insights into  $\text{CO}_2$ -based geochemical reactions that may occur, for example, during carbon capture, utilization, and storage operations.

### 1. INTRODUCTION

Fluid-rock reactions involved in fluid injections into hot reservoirs are of crucial importance in many geo-engineering systems, such as enhanced geothermal systems (EGS) (Althaus and Edmunds, 1987; Pandey et al., 2015) and carbon capture, utilization, and storage (CCUS) (Guas, 2010; Xu et al., 2003). These geochemical reactions lead to mineral dissolution and precipitation which may change the hydraulic, mechanic, thermal and chemical properties of the reservoir. When multiple minerals are present in the reservoir, different reactions are more or less dominant, depending on the reaction rates. When a mineral is actively participating in these surface reactions (e.g. mineral dissolution and precipitation), its involved surface area is defined as the so-called effective surface area (ESA) of this mineral, which is one of the key parameters that controls the rate of the reactions. However, in a multi-mineral heterogeneous porous medium, it is extremely challenging to accurately estimate the effective surface area (Beckingham *et al.*, 2016, 2017; Noiriel and Daval, 2017). On the one hand, the physically accessible surface area (ASA) of each individual mineral is difficult to determine. Whole rock Brunauer-Emmett-Teller (BET) measurements cannot provide the ASAs of individual minerals, while image-based methods are inherently limited by the image resolution and can thus not provide the variability in the surface roughness of different minerals. On the other hand, the contributions of those ASAs are highly heterogeneous, due to the large variation in the local pore-fluid chemistry and flow velocity.

In this study, we quantify the ESA of the dolomite cement ( $\text{Ca}_{1.05}\text{Mg}_{0.75}\text{Fe}_{0.2}(\text{CO}_3)_2$ ) in a multi-mineral sandstone from a geothermal formation. The physical ASA of each mineral phase is firstly determined as the product of the surface area calculated from scanned images and from the scaling factors (SFs) obtained through a Monte-Carlo algorithm. Then, a reactive flow-through experiment is performed on the same sandstone specimen under reservoir conditions, using  $\text{CO}_2$ -enriched brine. Effluents are collected and analyzed to estimate the dolomite dissolution rate and the ESA during the reaction.

### 2. METHODS

#### 2.1 Material

The rock specimens used in this study are sandstones taken from a depth of 954 m from Geothermal well Vydmantai-1 in Lithuania. The specimen consists of quartz, dolomite, k-feldspar, muscovite, kaolinite and ilmenite. Dolomite ( $\text{Ca}_{1.05}\text{Mg}_{0.75}\text{Fe}_{0.2}(\text{CO}_3)_2$ ) was found as the most reactive component in the sample, with a volume fraction of 12.22% mostly in the form of cement. The specimen has a porosity of 21.9% and a permeability of 300 mD. The total specific surface area of the sandstone specimen is measured to be  $1.67\ \text{m}^2/\text{g}$  by employing the BET method. A cylindrical core sample with a diameter of 25.4 mm and a length of 39 mm was prepared for the flow-through experiment, explained in detail in Section 2.4.

#### 2.2 Scanning electron microscope (SEM) images

Both backscatter electron (BSE) images and Energy Dispersive X-ray Spectroscopy (EDS) images were collected, employing a Jeol JSM-6390 LA scanning electron microscope (SEM) in the Electron Microscopy Lab of the High-pressure group at ETH Zurich. The scans covered a field of  $11.37\ \text{mm} \times 8.34\ \text{mm}$  ( $94.8\ \text{mm}^2$ ) on a thin section of the sandstone specimen. A gray-scale image, with a pixel resolution of  $1.2\ \mu\text{m}$  and a total pixel number of  $9474 \times 6947$ , was acquired from the BSE scan and a color-coded image with a pixel resolution of  $2.4\ \mu\text{m}$  and a total pixel number of  $4737 \times 3474$  was acquired from the EDS scan. The BSE image preserves good contrast and detailed structures of the pores, while the EDS image distinguishes different mineral phases, based on their element compositions. The two scanned images were registered with a Matlab script to generate a mineral distribution map (Figure 1).

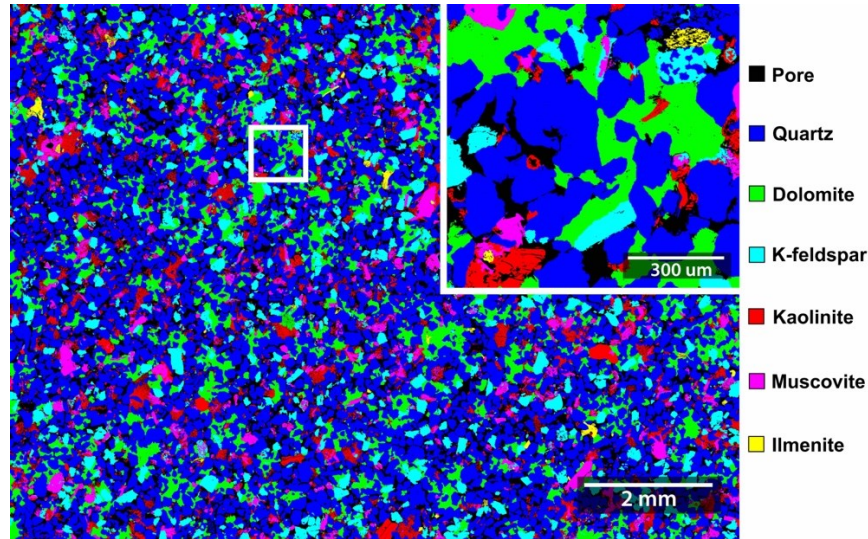


Figure 1: Registered SEM image, color coded for different minerals.

### 2.3 Calculation of mineral physical ASA

From each segmented mineral map, we first calculated the surface areas of individual minerals that are exposed to the pore space, i.e., the corresponding ASA. However, this ASA does not account for the surface roughness and other sub-pixel features that cannot be captured by the SEM image, due to the limited image resolution. Therefore, we determined the mineral-specific scaling factors (SF) proposed by a Monte-Carlo algorithm (Ma et al., 2019) to appropriately correct the ASA. We benchmark the sum of the corrected mineral ASAs against the BET measurement and the mineral single-grain surface area against the pure mineral BET values from the literature. The Monte-Carlo algorithm can search for the most probable SF for each mineral (Table 1). Then, the corrected physical ASA for each mineral is obtained by multiplying the image-calculated ASA by the corresponding SF.

Table 1: The ASAs obtained from the SEM image, the scaling factors (SF), applied to the ASAs and the corrected ASAs

	Quartz	Dolomite	K-feldspar	Muscovite	Kaolinite	Ilmenite
ASA from image (m <sup>2</sup> /g)	0.0173	0.0030	0.0034	0.0038	0.0149	0.0004
SF	7.00	21.79	3.09	30.90	91.00	3.69
Corrected ASA (m <sup>2</sup> /g)	0.121	0.065	0.011	0.117	1.356	0.001

### 2.4 Reactive flow-through experiment

A reactive flow-through experiment was performed on the same sandstone specimen in the laboratory of the Geothermal Energy and Geo fluids Group at ETH Zürich. Figure 2 shows the flow-through experiment setup, which consists of a triaxial reaction cell, a heating system, a central controlling system, 4 syringe pumps, and 2 effluent sampling apparatuses. The sandstone specimen was placed vertically in the center of the triaxial cell. The cell can be heated up to a desired temperature ( $\leq 200$  °C) by the heating system with an electric heating jacket around the triaxial cell. Two hastelloy-coated volumetric syringe pumps recycled the working fluid through the sandstone specimen at a desired flow rate and back pressure. The recycling of working fluids was continuously regulated by a synchronization program that controls the working mode of the recycling pumps and the open-and-shut status of the corresponding electronic valves. During one injection cycle, one of the recycling pumps served as an injection pump, providing a constant fluid flow rate, while the other recycling pump served as a collection pump, providing a constant back pressure. An injection cycle ended when the fluid volume of the injection pump was less than a set value, and the next cycle began simultaneously after switching between the collection and the injection pumps. The flow direction through the core did not change during the switching because of the redirection of the flow using corresponding electronic valves. A CO<sub>2</sub>-enriched brine (0.8 mol/L CO<sub>2</sub> and 1 mol/L NaCl) was circulated through the specimen at a constant flow rate of 2 ml/min for the first 42 cycles and 1 ml/min for the rest of the cycles at a pressure of 100 bar and a temperature of 40 °C, according to the reservoir conditions. Effluents from both the fluid inlet and the outlet were collected and the concentration of the major dissolved cations were determined by means of inductively coupled plasma optical emission spectrometry (ICP-OES) in the Laboratory of Inorganic Chemistry at ETH Zürich.

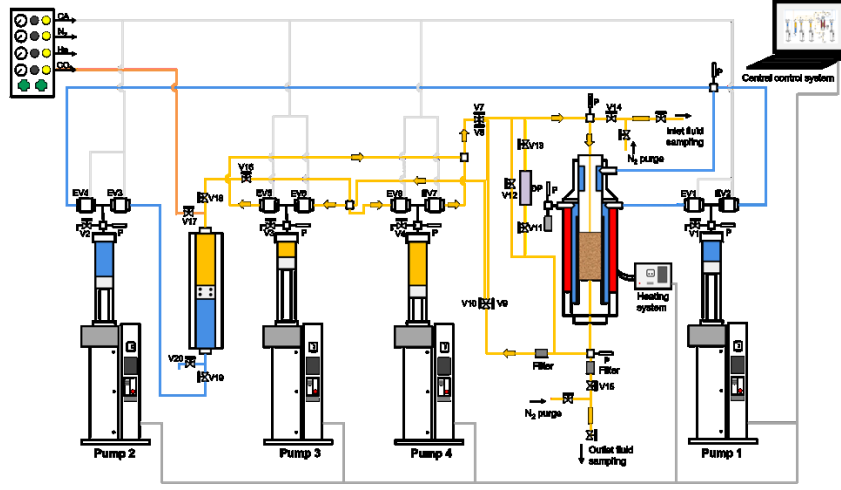


Figure 2: Sketch of the reactive flow-through system.

### 2.5 Calculating ESA

Knowing the concentration of the major cations, calcium in particular, we can deduce the reactivity of dolomite ( $\text{mol m}^{-3} \text{s}^{-1}$ ) using:

$$\overline{R(t)} = \frac{\Delta C(t)Q}{xV_{sd}} \quad (1)$$

where  $\Delta C$  is the calcium concentration difference between the fluid inlet and the outlet,  $Q$  is the volumetric injection rate ( $\text{ml/min}$ ),  $x$  is the stoichiometric coefficient of calcium in dolomite ( $x=1.05$ ), and  $V_{sd}$  is the bulk volume of the cylindrical specimen (Ma et al., 2019). Furthermore, the surface area participating in the dolomite dissolution reaction can be obtained using

$$\overline{R(t)} = \bar{r}e(t)\bar{S}(t)\rho_{rock}(1 - \bar{\Omega}(t)) \quad (2)$$

where  $\bar{r}$  ( $\text{mol m}^{-2} \text{s}^{-1}$ ) is the dolomite surface reaction rate constant,  $\bar{\Omega}$  is the sample-averaged saturation state,  $\bar{S}$  ( $\text{m}^2/\text{g}$ ) is the sample-averaged ASA of the corresponding mineral (Table 1),  $\rho_{rock}$  is the bulk density of the specimen, and  $e$  is a coefficient that describes the efficiency of the accessible SSA during the reaction. The cation concentrations from the fluid inlet and the outlet are fairly close, due to a high flow rate used in the experiment. Therefore, the calculated effective SSA,  $ESA = e\bar{S}$ , represents the actual reacting surface, located mainly in the fast channels.

### 3 RESULTS AND DISCUSSION

Major cations found in the fluid samples include calcium, magnesium, iron, potassium, and aluminum. We use the concentration of calcium to calculate the reactivity of dolomite using Eq. (1), as shown in Figure 3. The reactivity declines rapidly during the first hours and then slowly reaches a rate as low as  $0.2 \text{ mmol m}^{-3} \text{s}^{-1}$ . When the flow rate is changed from  $2 \text{ ml/min}$  to  $1 \text{ ml/min}$ , a sharp drop in the reactivity can be observed. This drop could be caused by the flow field change, which leads to the spreading of the stagnation zone.

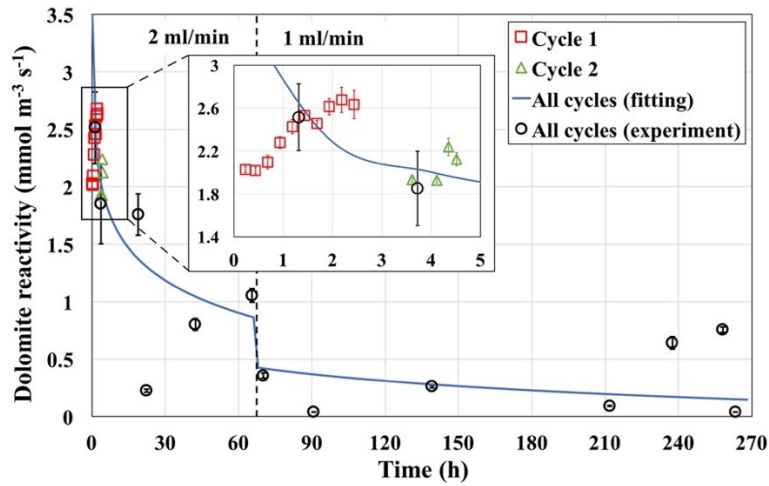


Figure 3: Evolution of dolomite reactivity with an enlargement for the first two cycles. The solid line is calculated by the regressed Ca concentration.

The ESA of dolomite was then calculated using Eq. (2) and plotted in Figure 4 (Ma et al, 2019). The ESA is found to increase at the beginning of the experiment, despite dolomite reactivity decreasing, due to a sharp drop of the surface reaction rate. Later on, the ESA declines slowly, except for a step-like drop during the change of flow rates. The calculated dissolved dolomite volume is also shown in Figure 4, indicating that the dissolution reaction mainly occurred during the first 90 hours.

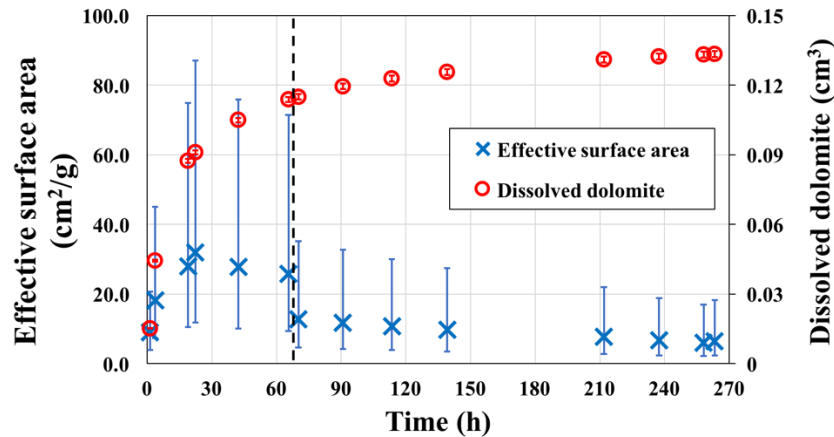


Figure 4: Evolution of the ESA (blue cross) and the dissolved volume (red circle) of dolomite.

#### 4 CONCLUSIONS

This study provides a potential method to effectively estimate the accessible surface area (ASA) of a mineral in a multi-mineral sandstone specimen and to predict the evolution of the effective surface area (ESA) during fluid-rock reactions. This approach enables the possibility of upscaling the changes in the ESA from the laboratory core scale to field-scale reactive transport simulations, thereby potentially shedding light on a wide range of geochemical processes that involve fluid-rock interface reactions.

#### ACKNOWLEDGMENTS

This work was supported by the ‘Demonstration of soft stimulation treatments of geothermal reservoirs (DESTRESS)’ project, funded by the European Union’s Horizon 2020 research and innovation program under Grant No. 691728. The Werner Siemens Foundation (Werner Siemens-Stiftung) is thanked by M.O. Saar for its support of the Geothermal Energy and Geofluids (GEG) Group (GEG.ethz.ch) at ETH Zurich. The rock sample was provided by the Lithuanian geothermal energy company Geoterma. We also thank N. Knornschild for his invaluable technical contributions in the GEG group.

#### REFERENCES

- Althaus, E, Edmunds, W.M.: Geochemical research in relation to hot dry rock geothermal systems, *Geothermics*, **16** (1987), 451-458.
- Beckingham, L. E. et al. Evaluation of mineral reactive surface area estimates for prediction of reactivity of a multi-mineral sediment, *Geochimica et Cosmochimica Acta*, **188** (2016), 310–329.
- Beckingham, L. E. et al.: Evaluation of accessible mineral surface areas for improved prediction of mineral reaction rates in porous media, *Geochimica et Cosmochimica Acta*. Elsevier Ltd, **205** (2017), 31–49.
- Gaus, I.: Role and impact of CO<sub>2</sub>–rock interactions during CO<sub>2</sub> storage in sedimentary rocks. *International Journal of Greenhouse Gas Control*, **4** (2010), 73–89.
- Ma, J. Querci, L., Hattendorf, B., Saar, O.M., Kong, X.Z.: Dolomite dissolution in sandstone by CO<sub>2</sub>-enriched brine circulation: Introducing a stochastic analysis on mineral ESA evolution. Submitted to *Environmental science & technology* (2019).
- Ma, J., Saar, O.M., Kong, X.Z.: A Monte-Carlo approach for the under-determined mineral-specific accessible surface area quantification. Submitted to *Chemical geology* (2019).
- Noiriell, C. and Daval, D.: Pore-Scale Geochemical Reactivity Associated with CO<sub>2</sub> Storage: New Frontiers at the Fluid-Solid Interface, *Accounts of Chemical Research*, **50** (2017), 759–768.
- Pandey, S.N., Chaudhuri, A., Rajaram, H., et al.: Fracture transmissivity evolution due to silica dissolution/precipitation during geothermal heat extraction, *Geothermics*, **57** (2015), 111–126.
- Xu, T.F., Apps, J.A., Pruess, K.: Reactive geochemical transport simulation to study mineral trapping for CO<sub>2</sub> disposal in deep arenaceous formations, *Journal of Geophysical Research-Solid Earth*, **108** (2003).